An Autosomal Dominant Bull's-Eye Macular Dystrophy (MCDR2) that Maps to the Short Arm of Chromosome 4

Michel Michaelides,[1] *Samantha Johnson,*[1] *Arabella Poulson,*[2] *Keith Bradshaw,*[2] *Caren Bellmann,*[1] *David M. Hunt,*[1] *and Anthony T. Moore*[1]

Purpose. To describe the phenotype of an autosomal dominant macular dystrophy and identify the chromosomal locus.

Methods. Eleven members of a five-generation, nonconsanguineous British family were examined clinically and also underwent automated perimetry, electrodiagnostic testing, fundus fluorescein angiography, and fundus autofluorescence imaging. Blood samples were taken for DNA extraction and linkage analysis was performed.

Results. The phenotype is characterized by bull's-eye macular dystrophy first evident in the first or second decade of life. There is mild visual impairment, central scotomata, and electrophysiological testing indicates that most affected individuals have disease confined to the central retina but older subjects have more widespread rod and cone abnormalities, demonstrated by flash ERG. Genetic linkage analysis established linkage to chromosome 4 at p15.2-16.3 with a maximum lod score of 3.03 at a recombination fraction of 0.00 for marker *D4S391*. The locus for this autosomal dominant macular dystrophy lies between flanking markers *D4S3023* and *D4S3022*, and overlaps the Stargardt 4 locus.

Conclusions. A new locus was identified for a bull's-eye macular dystrophy on the short arm of chromosome 4. (*Invest Ophthalmol Vis Sci.* 2003;44:1657–1662) DOI:10.1167/iovs.02-0941

The hereditary central receptor dystrophies are characterized by bilateral visual loss and the finding of generally symmetrical macular abnormalities on ophthalmoscopy. The age of onset is variable, but it appears in most affected individuals in the first two decades of life. There is considerable clinical and genetic heterogeneity. Macular dystrophies showing autosomal dominant, autosomal recessive, X-linked recessive, and mitochondrial inheritance have all been reported, and there is considerable heterogeneity even within these subtypes.[1,2] Several causative genes have now been identified (Table 1), but more remain to be discovered.

Age-related macular degeneration (ARMD) may also have a significant genetic component in its etiology. Approximately 20% of patients have a positive family history,[17] and twin studies support a strong genetic component.[18] Putative susceptibility loci have been identified on 1q25-31[19] and 17q25,[20] and it has been recently suggested that the e4 allele of the apolipoprotein E gene may have a protective effect on risk of ARMD.[21] Genes implicated in monogenic macular dystrophies are potential candidates for genes conferring risk for ARMD, although to date, with the possible exception of *ABCA4*, none of these genes has been shown to confer increased risk of ARMD.

In the present study we identified a locus on the short arm of chromosome 4 (4p) in a family with a dominantly inherited macular dystrophy in which there is a relatively mild phenotype.

Patients and Methods

A five-generation family with an autosomal dominant macular dystrophy was ascertained. The protocol of the study adhered to the provisions of the Declaration of Helsinki. After informed consent was obtained, a full ophthalmic examination was performed, blood samples were collected for DNA extraction, and linkage analysis was performed.

Clinical Assessment

Eleven members of a five-generation, nonconsanguineous British family were examined (Fig. 1). Although there was no male-to-male transmission, males and females were equally affected, and autosomal dominant inheritance is thought to be most likely. A full medical and ophthalmic history was obtained and an ophthalmic examination performed. Color vision testing was performed with Hardy, Rand, Rittler (HRR) plates (American Optical Company, New York, NY). Affected subjects also underwent automated visual field perimetry (Humphrey Perimeter; Humphrey Systems, Dublin, CA), color fundus photography, and fundus autofluorescence imaging with a confocal scanning laser ophthalmoscope (cSLO) (Zeiss prototype; Carl Zeiss Inc., Oberkochen, Germany). Electrodiagnostic assessment included an electro-oculogram (EOG), a flash electroretinogram (ERG), and pattern ERG (PERG), according to the protocols recommended by the International Society for Clinical Electrophysiology of Vision.[22–24] Patients IV:2 and V:1 underwent fundus fluorescein angiography (FFA).

The disease was diagnosed in individuals on the basis of the presence of macular abnormality and in most cases decreased visual acuity of variable severity.

Linkage Analysis Method

Genotyping. Genotyping was performed using markers from commercial linkage mapping sets (ABI MD-10 and HD-5, ver. 2.0; Linkage Mapping Sets; Applied Biosystems, Foster City, CA). These sets allow approximately 10- and 5-cM resolution of the human genome, respectively, and consist of fluorescence-labeled PCR primer pairs for 800 highly polymorphic dinucleotide repeat microsatellite markers chosen from a human linkage map provided by Gènèthon (www.genethon.fr; provided in the public domain by the French Association against Myopathies, Evry, France).[25–27]

PCR reactions were performed for each marker individually in a 5-μL reaction volume, containing 25 ng DNA, 15 mM Tris-HCl (pH 8.0),

From the [1]Institute of Ophthalmology, University College London, London, United Kingdom; and the [2]Department of Ophthalmology, Addenbrooke's Hospital, Cambridge, United Kingdom.

Supported by grants from the British Retinitis Pigmentosa Society and the Guide Dogs for the Blind Association.

Submitted for publication July 16, 2002; revised October 8, 2002; accepted November 7, 2002.

Disclosure: **M. Michaelides**, None; **S. Johnson**, None; **A. Poulson**, None; **K. Bradshaw**, None; **C. Bellmann**, None; **D.M. Hunt**, None; **A.T. Moore**, None

The publication costs of this article were defrayed in part by page charge payment. This article must therefore be marked "*advertisement*" in accordance with 18 U.S.C. §1734 solely to indicate this fact.

Corresponding author: Anthony T. Moore, Institute of Ophthalmology, University College London, 11-43 Bath Street, London, EC1V 9EL, UK; tony.moore@ucl.ac.uk.

TABLE 1. Chromosomal Loci and Causative Genes in Macular Dystrophies

Macular Dystrophy: OMIM Number	Mode of Inheritance	Chromosome Locus	Mutated Gene
Stargardt disease/fundus flavimaculatus; 248200[3]	Autosomal recessive	1p21-p22 (STGD1)	*ABCA4*
Stargardt-like macular dystrophy; 600110[4]	Autosomal dominant	6q14 (STGD3)	*ELOVL4*
Stargardt-like macular dystrophy; 603786[5]	Autosomal dominant	4p (STGD4)	Not identified
Adult vitelliform dystrophy; 179605[6]	Autosomal dominant	6p21.2-cen	*Peripherin/RDS*
Pattern dystrophy; 169150[7]	Autosomal dominant	6p21.2-cen	*Peripherin/RDS*
Best macular dystrophy; 153700[8]	Autosomal dominant	11q13	*VMD2*
Sorsby's fundus dystrophy; 136900[9]	Autosomal dominant	22q12.1-q13.2	*TIMP3*
Juvenile retinoschisis; 312700[10]	X-linked	Xp22.2	*XLRS1*
North Carolina macular dystrophy; 136550[11]	Autosomal dominant	6q14-q16.2 (MCDR1)	Not identified
Central areolar choroidal dystrophy; 215500[12,13]	Autosomal dominant	6p21.2-cen	*Peripherin/RDS*
		17p13	Not identified
Progressive bifocal chorioretinal atrophy; 600790[14]	Autosomal dominant	6q14-q16.2	Not identified
Doyne honeycomb retinal dystrophy; 126600[15]	Autosomal dominant	2p16	*EFEMP1*
Dominant cystoid macular dystrophy; 153880[16]	Autosomal dominant	7p15-p21	Not identified

50 mM KCl, 2.5 mM $MgCl_2$, 250 μM each dNTP, 1.25 pmol each primer and 0.25 U *Taq* polymerase (*AmpliTaq* Gold; Applied Biosystems). Reactions were performed on a thermocycler (model 9600; Perkin Elmer, Wellesley, MA) with a standard thermocycling profile for all markers. This consisted of an initial denaturation of 12 minutes immediately followed by 10 cycles of 95°C for 15 seconds, 55°C for 15 seconds, and 72°C for 30 seconds and then by 20 cycles of 89°C for 15 seconds, 55°C for 15 seconds, and 72°C for 30 seconds, with a single final extension step of 72°C for 10 minutes.

PCR products for selected sets of markers were pooled, diluted, and denatured in formamide and size fractionated using a gene analyzer (ABI 3100; Applied Biosystems). PCR products were automatically sized by the accompanying software (3100 Data Collection Software, ver. 1.0.1; Applied Biosystems), with *ROX* used as the size

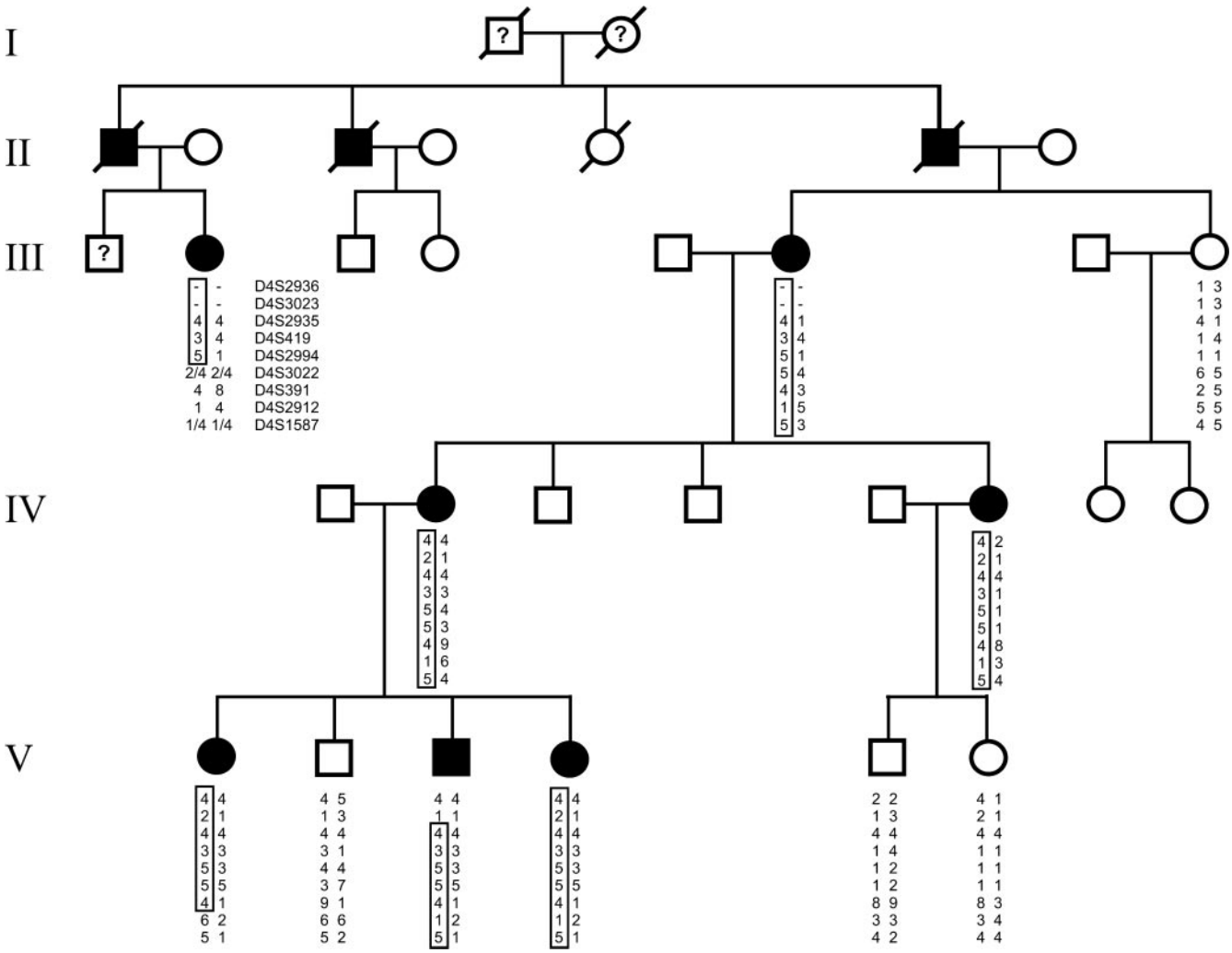

FIGURE 1. Five-generation pedigree of a family with autosomal dominant macular dystrophy. The alleles present for each of the nine chromosome 4p microsatellite markers used are shown. The minimal disease region for each affected individual is boxed.

standard, and scored by using GeneMapper (version 2.0; Applied Biosystems). Data were checked for genotyping errors using PedCheck (developed by Jeff O'Connell, University of Pittsburgh, Pittsburgh, PA).[28]

Linkage Analysis. Subjects were classified as affected, unaffected, or status unknown according to their clinical status. Linkage analysis was performed by using standard lod score methods. Two point lod scores were calculated using the MLINK program of the LINKAGE (ver. 5.1) package (http:www.hgmp.mrc.ac.uk/; provided in the public domain by the Human Genome Mapping Project Resources Center, Cambridge, UK).[29] A fully penetrant dominant model with a disease allele frequency of 0.0001 was assumed. Marker allele frequencies were assumed to occur at equal frequencies, because population allele frequencies were not available.

Results

The disorder was identified in a five-generation British family as shown in Figure 1.

Patient V:1

A 17-year-old woman (the proband) was first examined at age 13 having noticed blurred vision when reading and metamorphopsia. This difficulty with reading had gradually worsened. There were no reported problems with night vision. Visual acuity was 6/9 bilaterally. HRR testing revealed a mild red-green defect and medium tritan defect bilaterally. Dilated fundoscopy revealed bilateral macular retinal pigment epithelium (RPE) mottling and atrophy with fine perifoveal red granular patches. Visual fields demonstrated mildly reduced central sensitivity. Fundus autofluorescence revealed a ring of moderately increased perifoveal autofluorescence bilaterally. Fluorescein angiography showed localized masking of the choroidal fluorescence in the perifoveal area. The PERG P50 component was mildly subnormal. EOG and flash ERG were normal.

Patient V:3

This 9-year-old boy had occasional difficulty with reading small print. Visual acuity was 6/6 bilaterally. HRR revealed mild red-green defect bilaterally. Fundoscopy revealed a bilateral prominent foveal reflex and a red-speckled appearance at the level of the RPE. Fundus autofluorescence revealed a mild perifoveal ring of increased autofluorescence. The ERG was normal. PERG and EOG were not performed because of poor cooperation.

Patient V:4

This 14-year-old girl was asymptomatic, except for noticing some difficulty with color vision, especially the color blue. Visual acuity was found to be 6/5 bilaterally. Color testing with HRR plates revealed a mild tritan and red-green defect in the left eye and normal color vision on the right. Fundus examination revealed a mild abnormality of the macula with bilateral red-speckled appearance at the level of the RPE, more prominent in the left than the right eye. There was once again a prominent foveal reflex bilaterally. Fundus autofluorescence was unremarkable. PERG, ERG, and EOG were normal.

Patient IV:2

This 41-year-old woman reported glare at night but was otherwise asymptomatic. Visual acuity was 6/5 bilaterally. Color vision assessment with the HRR plates revealed generalized dyschromatopsia affecting protan, deutan, and tritan axes. Fundoscopy revealed bilateral macular RPE mottling with a dark red perifoveal region (Fig. 2A). Visual field testing revealed bilateral central scotomata. Fundus autofluorescence imaging revealed bilateral bull's-eye lesions, comprising a ring of decreased perifoveal autofluorescence bordered peripherally and centrally (to a lesser extent) by increased autofluorescence (Fig. 2B). Fluorescein angiography revealed masking of the choroidal fluorescence in the perifoveal area (Fig. 2C). There was no recordable PERG, but EOG and ERG were normal.

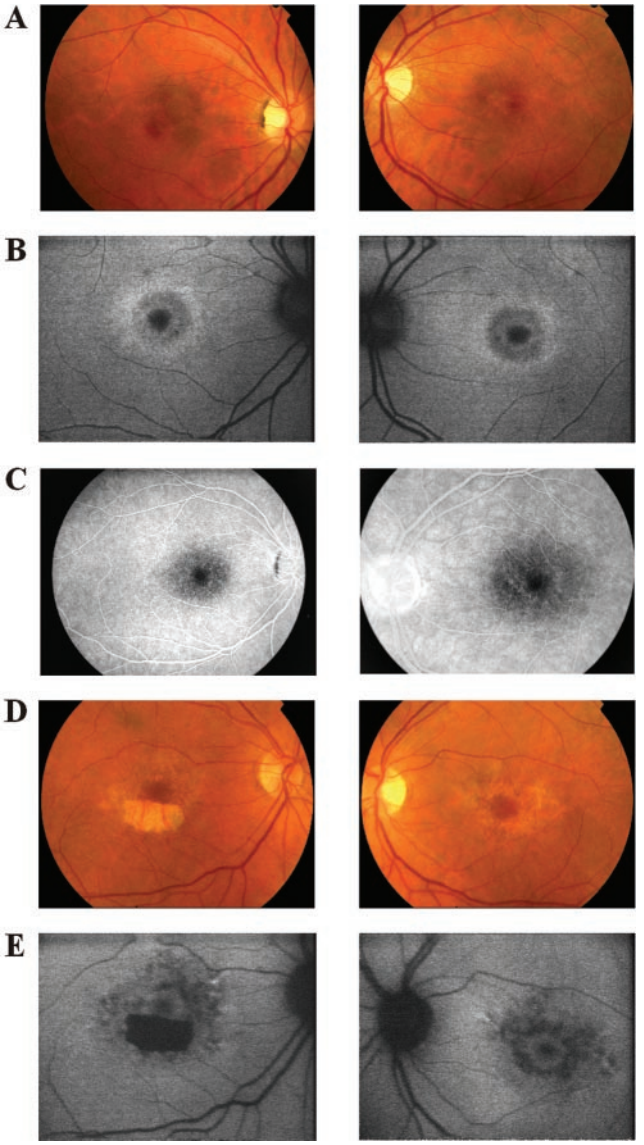

Figure 2. (**A**) Patient IV:2: fundus photograph showing bilateral RPE mottling and temporal optic disc pallor. (**B**) Patient IV:2: fundus autofluorescence imaging revealed bilateral bull's-eye–type lesions, comprising a ring of decreased perifoveal autofluorescence bordered peripherally and centrally by increased autofluorescence. (**C**) Patient IV:2: fluorescein angiography showing bilateral localized masking of the choroidal fluorescence in the perifoveal area. (**D**) Patient III:6: fundus photography showing bilateral bull's-eye maculopathy, with a well-demarcated area of RPE atrophy at the right macula, and bilateral temporal optic disc pallor. (**E**) Patient III:6: fundus autofluorescence imaging revealed bilateral bull's-eye type lesions, more prominent in the left than the right.

Patient IV:6

This 37-year-old woman had light sensitivity and reported glare at night. She had a visual acuity of 6/5 bilaterally and color vision was normal. Fundoscopy revealed subtle bilateral foveal abnormalities, with central pallor and surrounding mottling of

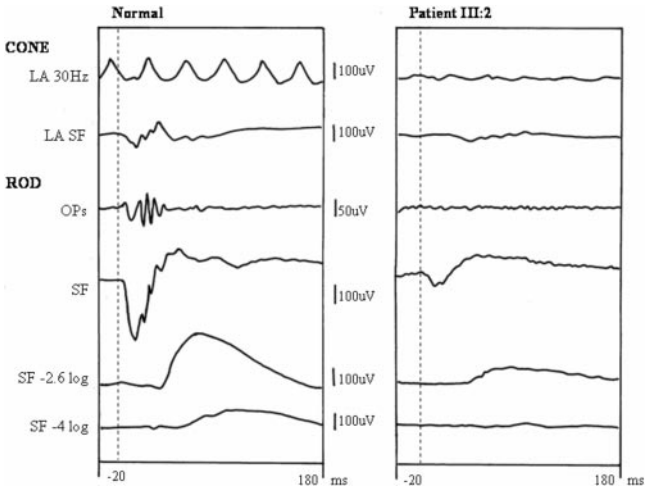

FIGURE 3. The flash ERG of Patient III:2, compared to normal control (*left*), showed reduced scotopic and photopic responses. LA, light adapted; SF, standard flash (ISCEV Clinical ERG Standard); OPs, oscillatory potentials. *Broken line*: time of stimulus flash.

the RPE. Fundus autofluorescence showed an increased signal in the perifoveal region. Visual field testing was within normal limits. The PERG P50 component revealed low-amplitude responses on the right and borderline abnormality on the left. EOG and flash ERG were normal.

Patient III:2

This 63-year-old woman was first seen at age 24, reporting difficulty with reading and bilateral central visual field defects. Visual field testing at first presentation with Bjerrum's tangent screen revealed bilateral central scotomata. Visual acuity at that time was 6/4 bilaterally. Granular pigmentation was noted at both maculae. Over a period of 35 years, visual acuity had gradually deteriorated to 6/24 in the right eye and 6/36 in the left. Fundoscopy revealed a bull's-eye maculopathy. The PERG was unrecordable from either eye. Rod and cone flash ERG responses were subnormal, suggesting a more widespread retinal dysfunction with disease progression (Fig. 3). EOG was not possible because of lack of cooperation.

Patient III:6

This 61-year-old woman was first seen at age 12 after having some difficulty with reading vision and light sensitivity. She thought that her vision was slow to adapt to dim illumination. Visual acuity was 6/6 in her right eye and 6/9 in her left. Color vision testing yielded normal results. Dilated fundoscopy revealed bilateral RPE mottling, with a well-demarcated area of RPE atrophy at the right macula (Fig. 2D). She had bilateral central scotomata on visual field testing. Fundus autofluorescence imaging revealed bilateral bull's-eye lesions, which consisted of a ring of decreased perifoveal autofluorescence bordered peripherally (to a lesser extent) and centrally by increased autofluorescence (Fig. 2E). The PERG was unrecordable. EOG was normal, but the rod and cone flash ERG responses were subnormal.

Patients V:2, V:5, V:6, IV:3, and III:8

These patients were also assessed and were found to be asymptomatic, with clinical examination producing entirely normal findings.

Linkage Studies

Markers previously known to be linked to Stargardt disease (STGD) and cone–rod dystrophy (CORD) were examined in the first instance. No significant linkage was found in the following chromosome regions: *CORD6* on 17p,[30] *CORD7* on 6q,[31] *CORD8* on 1q,[32] *GCAP* on 6p,[33] *STGD1* on 1p,[3] and *STGD3* on 6q.[4] In total approximately 50% of the genome was screened involving genotyping of 195 markers before significant linkage was established to 4p15.2-16.3 with a maximum lod score of 3.03 at a recombination fraction of 0.00 for marker *D4S391* (Table 2).

Recombination in patients III:2 and V:3 (Fig. 1) identifies the flanking markers for this dominant macular dystrophy as *D4S3022* and *D4S3023*, a genetic distance of 32 cM.

DISCUSSION

We have mapped an autosomal dominant macular dystrophy to 4p15.2-16.3. According to the convention established by the nomenclature used for North Carolina macular dystrophy phenotype (MCDR1), we have termed this disorder MCDR2 (MC, macular; D, dystrophy; R, retinal). The macular dystrophy in this family is of early onset, and in most affected individuals the disease is confined to the macular region. The early macular abnormalities include an increased foveal reflex and a red-speckled macular appearance, progressing to a more classic bull's-eye maculopathy. Fluorescein angiography performed in two subjects with early disease showed hypofluorescence in the perifoveal area suggestive of accumulation in the RPE of an abnormal material that masks choroidal fluorescence. Older individuals have electrophysiological evidence of more widespread retinal dysfunction.

The term bull's-eye maculopathy (BEM) was first introduced to describe the characteristic appearance of chloroquine retinopathy.[34] Bull's-eye lesions have since been reported in cone dystrophy and CORD,[35] rod–cone dystrophy,[36] and in some forms of macular dystrophy.[37–39] The pathogenesis of BEM is poorly understood. The characteristic appearance in which there is annular RPE atrophy, and central sparing may correspond to the pattern of lipofuscin accumulation in the RPE, which in healthy individuals is highest at the posterior pole and shows a depression at the fovea.[40,41] The initially spared center usually becomes involved as the disease progresses.

Advances in ocular imaging have resulted in a new technique to visualize the RPE, taking advantage of its intrinsic fluorescence derived from lipofuscin.[42–44] Autofluorescence imaging with a cSLO can provide useful information about the distribution of lipofuscin in the RPE and give indirect information on the level of metabolic activity of the RPE which is largely determined by the rate of turnover of photoreceptor

TABLE 2. Lod scores between Autosomal Dominant Macular Dystrophy and Microsatellite Markers on 4p

	Lod Score at θ					
Marker	**0.00**	**0.05**	**0.10**	**0.20**	**0.30**	**0.40**
D4S2936	$-\infty$	−0.03	0.14	0.18	0.11	0.03
D4S3023	$-\infty$	−0.4	−0.22	−0.05	−0.02	−0.01
D4S2935	0.45	0.41	0.36	0.27	0.17	0.08
D4S419	1.44	1.27	1.09	0.76	0.44	0.18
D4S2994	2.30	2.05	1.79	1.28	0.79	0.36
D4S3022	−2.25	1.07	1.21	1.12	0.83	0.45
D4S391	3.03	2.76	2.47	1.87	1.24	0.61
D4S2912	$-\infty$	1.35	1.39	1.16	0.79	0.39
D4S1587	$-\infty$	0.46	0.24	0.31	0.25	0.14

outer segments.[44] There is evidence of continuous degradation of autofluorescent material in the RPE.[44] Progressive loss of lipofuscin occurs when there is reduced metabolic demand because of photoreceptor cell loss, and this may explain the decreased autofluorescence (AF) seen in areas of photoreceptor cell loss in eyes with retinitis pigmentosa and rod–cone dystrophies.[44] Areas of increased AF correspond to a group of RPE cells containing higher quantities of lipofuscin than their neighbors and may represent areas at high risk for photoreceptor cell loss.[40] It has been demonstrated histologically that the number of photoreceptor cells is reduced in the presence of increased quantities of lipofuscin in the RPE, leading to the proposal that autofluorescent material may accumulate before cell death.[45] Increased lipofuscin may reflect either increased outer segment turnover or the inability of the RPE to process outer segment debris. In our family concentric areas of increased AF at the macula were evident in some individuals before there was ophthalmoscopic evidence of retinal atrophy. This may suggest that the primary site of dysfunction is in the RPE, but the findings of a normal EOG indicate that there is no widespread RPE abnormality. Alternatively, the increased AF could occur as a result of primary disease of the photoreceptors, which in the early stages of the disease is confined to the macular region but becomes more widespread in the late stages.

In our family we established linkage to 4p15.2-16.3. This region contains the candidate gene *PROML1*, encoding human prominin (mouse)-like-1 which belongs to the prominin family of 5-transmembrane domain proteins. *PROML1* is expressed in retinoblastoma cell lines and adult retina, and the product of the mouse orthologue (prom) is concentrated in membrane evaginations at the base of the outer segments of rod photoreceptors. A homozygous mutation in *PROML1* has been identified in an Indian pedigree with autosomal recessive retinal dystrophy. The mutation results in the production of a truncated protein, and functional studies in transfected CHO cells have demonstrated that the truncated prominin protein fails to reach the cell surface, indicating that the loss of prominin may lead to retinal degeneration through impaired generation of evaginations or conversion to outer segment disks.[46]

A locus for an autosomal dominant Stargardt-like disease has also been mapped to the short arm of chromosome 4 (STGD4) in a Caribbean family.[5] Analysis of extended haplotypes localized the disease gene to a 12-cM interval between loci *D4S1582* and *D4S2397*. This interval overlaps with our defined MCDR2 region. However our pedigree differs considerably from that of the Caribbean family, in that neither of our patients who underwent FFA demonstrated the characteristic dark choroid pattern that was seen in the Caribbean patients and our patients did not have the retinal flecks that were prominent in the Stargardt-like pedigree. The macular dystrophy we report appears to be clinically distinct from the STGD4 disorder. Therefore, even if both disorders are allelic, it is likely that different mutations are involved in their etiology. An alternative explanation is that the two disorders are caused by mutations in two different adjacent genes on 4p. The true situation will be resolved only by the identification of the underlying genetic mutations.

Acknowledgments

The authors thank the patients who kindly agreed to take part in this study.

References

1. Moore AT, Evans K. Molecular genetics of central retinal dystrophies. *Aust NZ J Ophthalmol.* 1996;24:189–198.
2. Musarella M. Molecular genetics of macular degeneration. *Doc Ophthalmol.* 2001;102:165–177.
3. Allikmets R, Singh N, Sun H, et al. A photoreceptor cell-specific ATP-binding transporter gene (ABCR) is mutated in recessive Stargardt macular dystrophy. *Nat Genet.* 1997;15:236–246.
4. Zhang K, Kniazeva M, Han M, et al. A 5-bp deletion in *ELOVL4* is associated with two related forms of autosomal dominant macular dystrophy. *Nat Genet.* 2001;27:89–93.
5. Kniazeva M, Chiang MF, Morgan B, et al. A new locus for autosomal dominant Stargardt-like disease maps to chromosome 4. *Am J Hum Genet.* 1999;64:1394–1399.
6. Felbor U, Schilling H, Weber BHF. Adult vitelliform macular dystrophy is frequently associated with mutation in the peripherin/RDS gene. *Hum Mutat.* 1997;10:301–309.
7. Nichols BE, Drack AV, Vandenburgh K, et al. A 2 base pair deletion in the RDS gene associated with butterfly-shaped pigment dystrophy of the fovea. *Hum Mol Genet.* 1993;2:601–603.
8. Petrukhin K, Koisti MJ, Bakall B, et al. Identification of the gene responsible for Best macular dystrophy. *Nat Genet.* 1998;19:241–247.
9. Weber BH, Vogt G, Pruett RC, Stohr H, Felbor U. Mutations in the tissue inhibitor of metalloproteinases-3 (TIMP3) in patients with Sorsby's fundus dystrophy. *Nat Genet.* 1994;8:352–356.
10. Sauer CG, Gehrig A, Warneke-Wittstock R, et al. Positional cloning of the gene associated with X-linked juvenile retinoschisis. *Nat Genet.* 1997;17:164–170.
11. Small KW. North Carolina macular dystrophy: clinical features, genealogy, and genetic linkage analysis. *Trans Am Ophthalmol Soc.* 1998;96:925–961.
12. Reig C, Serra A, Gean E, et al. A point mutation in the RDS-peripherin gene in a Spanish family with central areolar choroidal dystrophy. *Ophthalmol Genet.* 1995;16:39–44.
13. Hughes AE, Lotery AJ, Silvestri G. Fine localisation of the gene for central areolar choroidal dystrophy on chromosome 17p. *J Med Genet*. 1998;35:770–772.
14. Kelsell RE, Godley BF, Evans K, et al. Localization of the gene for progressive bifocal chorioretinal atrophy (PBCRA) to chromosome 6q. *Hum Mol Genet.* 1995;4:1653–1656.
15. Stone EM, Lotery AJ, Munier FL, et al. A single EFEMP1 mutation associated with both Malattia Leventinese and Doyne honeycomb retinal dystrophy. *Nat Genet.* 1999;22:199–202.
16. Kremer H, Pinckers A, van den Helm B, et al. Localization of the gene for dominant cystoid macular dystrophy on chromosome 7p. *Hum Mol Genet.* 1994;3:299–302.
17. Klaver CC, Wolfs RC, Assink JJ, van Duijn CM, Hofman A, de Jong PT. Genetic risk of age-related maculopathy: population-based familial aggregation study. *Arch Ophthalmol.* 1998;116:1646–1651.
18. Meyers SM, Zachary AA. Monozygotic twins with age-related macular degeneration. *Arch Ophthalmol.* 1988;106:651–653.
19. Klein ML, Schultz DW, Edwards A, et al. Age-related macular degeneration: clinical features in a large family and linkage to chromosome 1q. *Arch Ophthalmol.* 1998;116:1082–1088.
20. Weeks DE, Conley YP, Tsai HJ, et al. Age-related maculopathy: an expanded genome-wide scan with evidence of susceptibility loci within the 1q31 and 17q25 regions. *Am J Ophthalmol.* 2001;132:682–692.
21. Klaver CC, Kliffen M, van Duijn CM, et al. Genetic association of apolipoprotein E with age-related macular degeneration. *Am J Hum Genet.* 1998;63:200–206.
22. Marmor MF, Zrenner E. Standard for clinical electroretinography (1994 update). *Doc Ophthalmol.* 1995;89:199–210.
23. Bach M, Hawlina M, Holder GE, et al. Standard for pattern electroretinography. International Society for Clinical Electrophysiology of Vision. *Doc Ophthalmol.* 2000;101:11–18.
24. Marmor MF, Zrenner E. Standard for clinical electro-oculography. International Society for Clinical Electrophysiology of Vision. *Arch Ophthalmol.* 1993;111:601–604.
25. Weissenbach J, Gyapay G, Dib C, et al. A second-generation linkage map of the human genome. *Nature* 1992;359:794–801.
26. Gyapay G, Morissette J, Vignal A, et al. The 1993–94 Généthon human genetic linkage map. *Nat Genet.* 1994;7:246–339.

27. Dib C, Faure S, Fizames C, et al. A comprehensive genetic map of the human genome based on 5,264 microsatellites. *Nature.* 1996; 380:152–154.
28. O'Connell JR, Weeks DE. PedCheck: a program for identification of genotype incompatibilities in linkage analysis. *Am J Hum Genet.* 1998;63:259–266.
29. Cottingham RW, Idury RM, Schaffer AA. Faster sequential genetic linkage computations. *Am J Hum Genet.* 1993;53:252–263.
30. Kelsell RE, Evans K, Gregory CY, et al. Localisation of a gene for dominant cone-rod dystrophy (CORD6) to chromosome 17p. *Hum Mol Genet.* 1997;6:597–600.
31. Kelsell RE, Gregory-Evans K, Gregory-Evans CY, et al. Localization of a gene (CORD7) for a dominant cone-rod dystrophy to chromosome 6q. *Am J Hum Genet.* 1998;63:274–279.
32. Khaliq S, Hameed A, Ismail M, et al. Novel locus for autosomal recessive cone-rod dystrophy CORD8 mapping to chromosome 1q12–q24. *Invest Ophthalmol Vis Sci.* 2000;41:3709–3712.
33. Payne AM, Downes SM, Bessant D, et al. A mutation in guanylate cyclase activator 1A (GUCA1A) in an autosomal dominant cone dystrophy pedigree mapping to a new locus on chromosome 6p21.1. *Hum Molec Genet.* 1998;7:273–277.
34. Kearns TP, Hollenhorst RW. Chloroquine retinopathy: evaluation by fluorescein angiography. *Arch Ophthalmol.* 1966;76:378–384.
35. Krill AE, Deutman AF, Fishman M. The cone degenerations. *Doc Ophthalmol.* 1973;35:1–80.
36. Fishman GA, Fishman M, Maggiano J. Macular lesions associated with retinitis pigmentosa. *Arch Ophthalmol.* 1977;95:798–803.
37. Deutman AF. Benign concentric annular macular dystrophy. *Am J Ophthalmol.* 1974;78:384–396.
38. O'Donnell FE, Welch RB. Fenestrated sheen macular dystrophy: a new autosomal dominant maculopathy. *Arch Ophthalmol.* 1979; 97:1292–1296.
39. Slagsvold JE. Fenestrated sheen macular dystrophy: a new autosomal dominant maculopathy. *Acta Ophthalmol* (*Copenh*). 1981;59:683–688.
40. von Rückmann A, Fitzke FW, Bird AC. Fundus autofluorescence in age related macular disease imaged with a scanning laser ophthalmoscope. *Invest Ophthalmol Vis Sci.* 1997;38:478–486.
41. Wing GL, Blanchard GC, Weiter JJ. The topography and age relationship of lipofuscin concentration in the retinal pigment epithelium. *Invest Ophthalmol Vis Sci.* 1978;17:601–607.
42. von Rückmann A, Fitzke FW, Bird AC. Distribution of fundus autofluorescence with a scanning laser ophthalmoscope. *Br J Ophthalmol.* 1995;79:407–412.
43. von Rückmann A, Fitzke FW, Bird AC. In vivo fundus autofluorescence in macular dystrophies. *Arch Ophthalmol.* 1997;115: 609–615.
44. von Rückmann A, Fitzke FW, Bird AC. Distribution of pigment epithelium autofluorescence in retinal disease state recorded in vivo and its change over time. *Graefes Arch Clin Exp Ophthalmol.* 1999;237:1–9.
45. Dorey CK, Wu G, Ebenstein D, Garsd A, Weiter JJ. Cell loss in the ageing retina: relationship to lipofuscin accumulation and macular degeneration. *Invest Ophthalmol Vis Sci.* 1989;30: 1691–1699.
46. Maw MA, Corbeil D, Koch J, et al. A frameshift mutation in prominin (mouse)-like 1 causes human retinal degeneration. *Hum Mol Genet.* 2000;9:27–34.